Extreme Mechanics Letters 52 (2022) 101616

Contents lists available at ScienceDirect

Extreme Mechanics Letters

journal homepage: www.elsevier.com/locate/eml

Network structure influences bulk modulus of nearly incompressible filled silicone elastomers

Christopher W. Barney [a,b,c], Matthew E. Helgeson [a,b,*], Megan T. Valentine [a,c,**]

[a] Materials Research Laboratory, University of California Santa Barbara, Santa Barbara, CA 93106-5121, United States of America
[b] Department of Chemical Engineering, Engineering II Building, University of California Santa Barbara, Santa Barbara, CA 93106-5080, United States of America
[c] Department of Mechanical Engineering, Engineering II Building, University of California Santa Barbara, Santa Barbara, CA 93106-5070, United States of America

ARTICLE INFO

Article history:
Received 15 September 2021
Received in revised form 12 January 2022
Accepted 12 January 2022
Available online 19 January 2022

MSC:
00-01
99-00

Keywords:
Poisson's ratio
Hydrostatic stress
Sol fraction
Crosslinking density

ABSTRACT

The bulk modulus is a fundamental elastic property that quantifies a material's resistance to changing volume and is critical in loading situations where significant hydrostatic stresses develop. Rubbery polymer networks represent a class of nearly incompressible materials whose bulk modulus is orders of magnitude larger than the tensile elastic modulus. The current physical understanding of the bulk modulus in nearly incompressible polymer networks suggests that it is insensitive to structural features of polymer networks, such as the network topology and spatial distribution of crosslinks and chains; however, there is a lack of experimental evidence available in the literature to thoroughly examine this understanding. In this work, radially confined compression is used to quantify the bulk modulus of silicone blends with variable crosslinking density and sol fraction. These measurements demonstrate that the bulk modulus is systematically altered when changing the network structure. Poisson's ratio of the silicone blends is also characterized. These findings provide a deeper understanding of the connection between bulk modulus and molecular structure of nearly incompressible polymer networks.

1. Introduction

Developing a physical understanding of the elastic properties of rubbery polymer networks is a foundational problem in polymer science. Connecting the elastic modulus E to network structure required contributions from many researchers over the last 80 years and has been largely successful [1–14]. The introduction of more complex network structures such as multinetwork gels [15], mechanochemically active networks [16], slide-ring gels [17], and bottlebrush elastomers [18] over the last 20 years have kept this an active field of study. While significant effort has been invested in understanding E, developing similar structure–property relationships for bulk modulus K and, by extension, Poisson's ratio ν for polymer networks has received limited attention.

The bulk modulus can be defined in terms of E and ν,

$$K = \frac{E}{3(1-2\nu)}, \tag{1}$$

and quantifies a material's resistance to changing volume [19]. K is critical in loading situations where the material response is influenced by hydrostatic stress which has been shown to be the case in the stiffness of confined elastic layers [20–25], failure and cavitation of elastomers [26,27], and during needle insertion and injection [28–32]. Theoretical treatment of K for polymer networks has been limited by the scarcity of available literature data that characterizes this property with both high precision and variable network structure.

Methods for measuring the bulk modulus largely fall into one of two categories and often require specialized instrumentation to achieve a high level of precision. The first category indirectly reports K by characterizing both E and volume changes during deformation to estimate ν. Techniques that fall into this category include dilatometry [33–40], strain gauge analysis [41,42], and digital image correlation (DIC) [43–47]. DIC and strain gauge analysis are the simplest methods to perform; however, they are limited in precision as it appears that ν can only be readily determined to the first three decimal points [45]. While dilatometry is capable of higher precision, measurements to estimate ν to 4 decimal points often involve hazardous fluids, such as mercury which has low compressibility and high thermal conductivity, during operation [33,39]. The second category includes techniques that directly quantify bulk modulus by applying a large hydrostatic

* Correspondence to: Engineering II Building, Room 3337, University of California, Santa Barbara, Santa Barbara, CA 93106-5080.
** Correspondence to: Engineering II Building, Room 2361C, University of California, Santa Barbara, Santa Barbara, CA 93106-5070.
E-mail addresses: helgeson@ucsb.edu (M.E. Helgeson), valentine@engineering.ucsb.edu (M.T. Valentine).

https://doi.org/10.1016/j.eml.2022.101616
2352-4316/

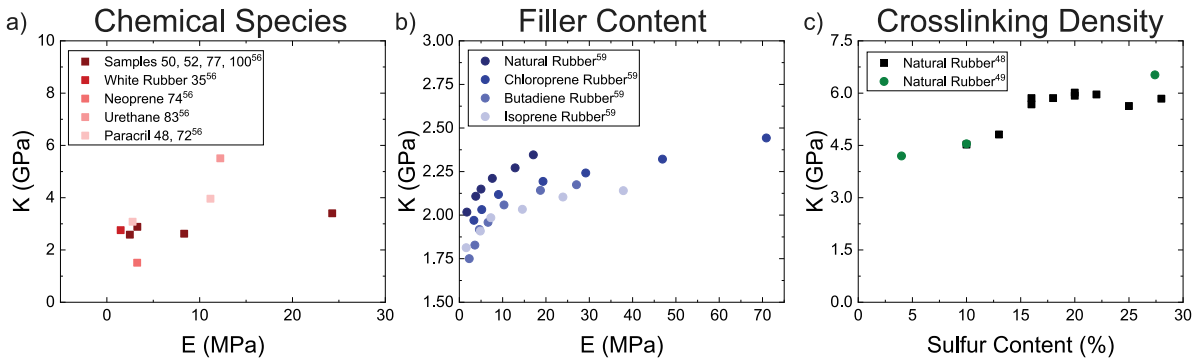

Fig. 1. Plots showing literature data measuring K against (a–b) E and (c) sulfur content while systematically altering material structure by changing (a) the chemical species tested, (b) filler content as well as pendant group on the backbone chain, and (c) crosslinking density. The data from Rightmire in (a) confirms Tabor's prediction that the identity of the chemical species impacts K [56]. The data of Holownia in (b) shows that the amount of carbon black filler added to rubber as well as the chemical identity of the pendant group of the rubber influences K [59]. The data of Adams and Bridgman [49] (green circles) and Weir [48] (black squares) in (c) shows that K is sensitive to the sulfur content in natural rubber samples. This data suggests that K should have a positive dependence on the crosslinking density. (For interpretation of the references to color in this figure legend, the reader is referred to the web version of this article.)

stress. This includes techniques that use a confining fluid to apply large pressures [48–58] as well as systems that exploit boundary conditions to convert large applied forces to hydrostatic stress [22,57–59]. The need to apply large pressures/forces in order to generate significant hydrostatic stress is a consequence of the nearly incompressible nature of most elastomers. For example, if $K = 1$ GPa then applying a 10% volumetric strain would require a pressure of 100 MPa (approximately 1000x greater than atmospheric pressure). Achieving the same pressure through constrained compression of a disk with a 1 cm radius would require 31.4 kN of force. Techniques in this category offer the highest level of precision and, under certain circumstances, can be used to estimate ν to the fifth decimal point [57]. These difficulties in precisely measuring K and ν have limited the physical understanding of these properties in rubbery networks.

Theoretical understanding of K and ν of polymer networks from a molecular perspective has been lacking. Previous attempts at modeling either of these properties have largely focused on the influence of filler particles [60] or time dependent viscoelasticity [61] by treating the material at the continuum scale. A notable exception is the model proposed by Tabor [19], who recognized that K of rubbery polymer networks, unlike E, is not entropic in nature and relates to intermolecular forces. Tabor modeled K of polybutadiene by representing two neighboring CH_2 groups along the polymer backbone as rigid spheres. This enabled calculating K by estimating the intermolecular forces that would resist compressing such spheres together,

$$K = \frac{1.8C}{a^9}, \tag{2}$$

where C is an interaction parameter from a Lennard-Jones type potential and a is the lattice spacing for a face-centered cubic (FCC) array of uniform spheres. As discussed in the SI, C and a can be estimated from the surface energy and molecular volume of the polymer. Eq. (2) was found to produce an estimate that was within a factor of 2 for a reference value [19].

While Tabor's model provided an adequate starting point for further models, it ignores the presence of structural features of polymer networks, including the network topology and density fluctuations, that are key in determining other elastic properties like E. The exclusion of these features is likely due to (1) the different physical origin of K relative to E and (2) the scarcity of available literature data that have quantified bulk modulus while systematically altering material structure. Bulk modulus data extracted from literature sources that have systematically altered material structure are shown in Fig. 1 [48,49,56,59]. Note that K is plotted against E as it is a conveniently measured mechanical property that has a well-established connection to network structure. However, this is not intended to suggest that K and E have similar physical origins. The data of Rightmire, shown in Fig. 1a as red squares, primarily alters the identity of the chemical species present by testing a number of commercial systems, confirming that molecular chemistry impacts K as Tabor suggested [56]. The data of Holownia, shown in Fig. 1b as blue circles, focuses instead on the chemistry of pendant groups on the backbone chain and amount of filler present in the system [59], where K increases with increasing filler content [59]. Both Adams and Gibson [49] as well as Weir [48] examined the impact of altering the crosslinking density of natural rubber; however, neither reported E for their samples and thus these data are plotted against the added sulfur content, which should scale directly with crosslinking density, in Fig. 1c. These data suggest a slight increase in K when increasing the crosslinking density. To the authors' knowledge, no experimental data set currently exists involving systematic alteration of the volume fraction of the polymer network. Based on these results, we hypothesize that the bulk modulus of an elastomer will vary as features of the network structure are systematically altered by tuning both the crosslinking density and volume fraction.

In the present work, this hypothesis is examined by characterizing K of silicone blends with variable crosslinking density and volume fractions through radially confined compression. First the methods and materials used in this experiment are presented. Then a discussion of E with particular care towards characterizing the sol fraction, defined as the fraction of polymer that is not anchored to the mechanically percolated network, is presented. This is then used to examine the relationship between K and E when altering network structure. Finally, a measurement of ν is presented alongside a discussion of the error in estimating this property. These findings represent a significant expansion of the bulk modulus data available in the literature and establish the measurements necessary to develop a more complete theoretical treatment of this property that considers network structure.

2. Methods and materials

2.1. Uniaxial extension

Uniaxial extension was used to determine E for samples. Force and displacement were monitored using a TA.XT Plus Connect Texture Analyzer with a 50 N load cell. Deformation of the samples was monitored using a Dino-Lite Edge Plus AM4117 series 1.3 MP camera. Samples were cut into rectangular strips (exact

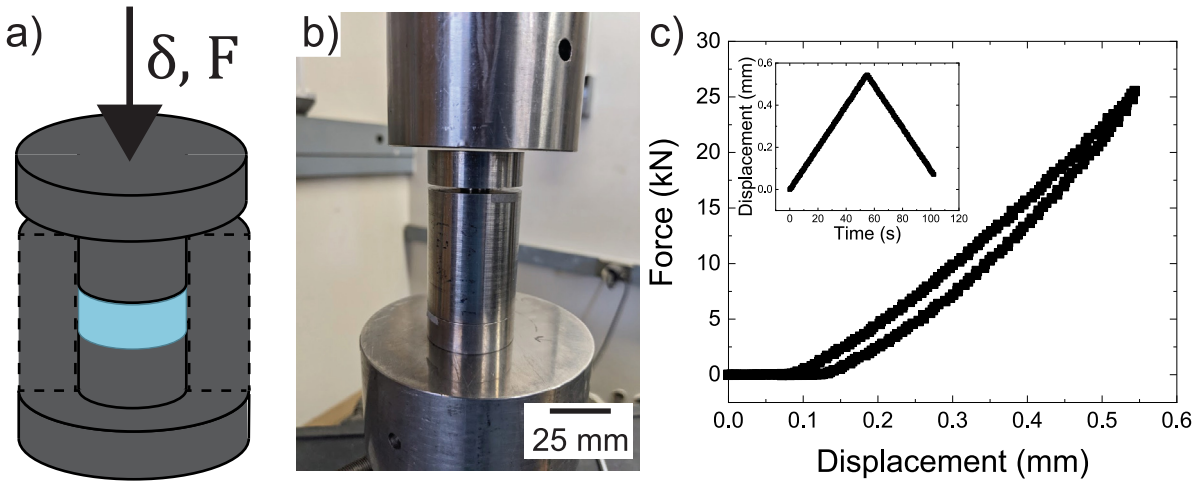

Fig. 2. (a) Sketch and (b) image showing the fixture used to perform radially confined compression, as well as (c) a plot of force vs. displacement with an inset showing displacement vs. time for a typical measurement.

Table 1
Gel fractions and E for the silicone blends used in this study. Sample refers to the sample name. Mixing ratio refers to the weight ratio of prepolymer base to curing agent. Weight fraction in linear chains refers to the weight fraction of Sylgard that is diluted with non-reactive short PDMS chains (approximately 6000 g/mol). Gel fraction ϕ refers to the measured gel fraction. Predicted ϕ refers to the predicted gel fraction if adding the chains acts as a simple diluent in the network. E refers to the value of Young's modulus measured via uniaxial extension. Note the close agreement between the observed gel fractions and those predicted by diluting the values measured for the undiluted samples suggesting that the presence of diluent does not significantly alter the network that forms. NA stands for not applicable.

Sample	Mixing ratio	Weight fraction in linear chains	Gel fraction ϕ	Predicted ϕ	E (kPa)
10:1-100	10:1	1	0.95	NA	2187
20:1-100	20:1	1	0.90	NA	617
30:1-100	30:1	1	0.79	NA	205
40:1-100	40:1	1	0.72	NA	91.3
10:1-875	10:1	0.875	0.84	0.83	1505
20:1-875	20:1	0.875	0.80	0.79	463
30:1-870	30:1	0.87	0.68	0.69	160
40:1-875	40:1	0.875	0.59	0.63	42.4
30:1-750	30:1	0.75	0.58	0.59	75.3
30:1-625	30:1	0.625	0.49	0.49	44.3
30:1-500	30:1	0.5	0.36	0.4	25.1

dimensions in supplementary table) and stretched with a displacement rate of 1 mm/s (approximately a strain rate of 0.025 s^{-1}) to a turnaround displacement of 25 mm (approximately a strain of 0.625). Summary data and plots showing these tests are contained in the SI.

2.2. Radially confined compression

Radially confined compression was used to determine K for the samples. Force and displacement were monitored using an MTS Model 810 Servo Hydraulic Universal Test Machine with a 100 kN load cell. Samples were punched into disks with a thickness of approximately 2 mm and a diameter of approximately 11.8 mm. Exact dimensions as well as summary data are available in the SI. Samples were compressed in a steel die, originally designed for powder compaction, at a displacement rate of 10 μm/s to a turnaround force of 25 kN. As shown in Fig. 2a–b, this setup consists of a cylindrical jacket and two sliding rams lubricated on the face and at the walls with a teflon spray. The inner and outer diameters of the jacket were 12 mm and 38.1 mm, respectively. The diameter of the rams was 11.9 mm leaving a 50 μm gap at the walls of the die. This gap was small enough to prevent material extrusion in most samples. The turnaround force was reduced for samples where extrusion was observed. Typical data gathered from this test are shown in Fig. 2c. The stiffness of the test fixture was measured at 153 MN/m and was used to extract the sample stiffness from the observed stiffness. Based on this geometry, it is possible to estimate a poroelastic relaxation time τ_{poro} during confined compression. [62] Taking a contact radius $a = 6$ mm and a diffusivity $D = 3.01 \times 10^{-12}$ m^2/s (estimated for migration of PDMS chains through a PDMS network) gives $\tau_{poro} = a^2/D \approx 10^7$ s. [63] This is significantly longer than the test time of approximately 100 s indicating that poroelasticity should not significantly contribute in this measurement. A summary of the data gathered with this technique is contained in the SI.

2.3. Materials

Silicone blends were used in order to probe the impact of network structure on bulk modulus. Samples were formed by mixing a commercially-available polydimethylsiloxane (PDMS) elastomer kit, Sylgard 184, with different prepolymer:curing agent ratios to alter the crosslinking density. Importantly, the prepolymer base component used in Sylgard 184 contains fumed silica as a filler. Literature estimates report the amount of silica filler in the range of 10–30 wt%. [64,65] Note also that changing the mixing ratio alters both the network crosslinking density and sol fraction. Hence, gel fractions ϕ, defined as the fraction of a polymer connected to the mechanically percolated network, were measured for each sample by swelling in excess toluene for seven days and are reported in Table 1. Samples used for swelling had cross-sectional dimensions of approximately 6 × 6 mm with a thickness of approximately 2 mm and no observation of fracture due to shrinkage stresses during the swelling and deswelling

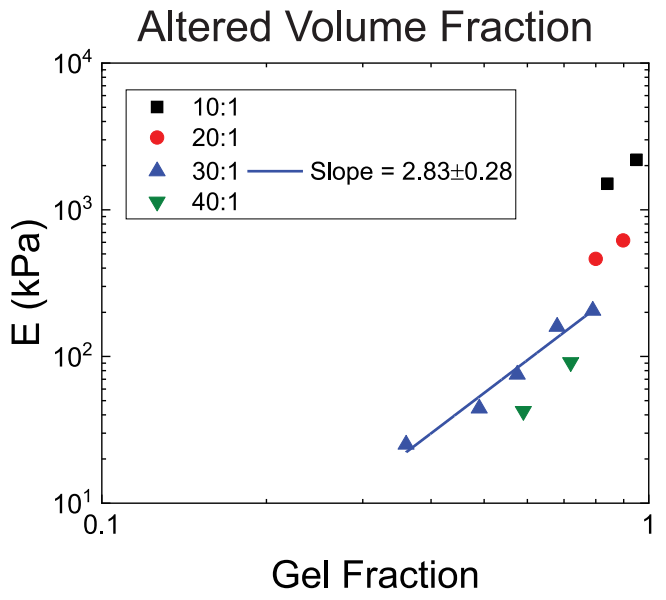

Fig. 3. Plot of E against gel fraction ϕ for sets of samples with different crosslinking densities, indicated by the mixing ratios. The 30:1 samples show that $E \sim \phi^{2.83\pm0.28}$ which may indicate a filler effect.

process was observed. To alter the volume fraction of the network formed, 100 cSt trimethylsiloxy terminated linear polydimethylsiloxane chains were added to the crosslinking system and mixed with the pre-cured material before crosslinking. The added PDMS chains are too short to form entanglements (approximately 6000 g/mol) and therefore act as a non-volatile, unreactive solvent. PDMS chains were chosen as a diluent because their chemical structure closely matches that of the PDMS network and should minimize any differences in the chemical species present in the system, which Tabor suggested would alter the bulk modulus [19]. Samples were mixed and then degassed under vacuum before films were cured at 70 °C for 21 h and then immediately removed and left to cool at room temperature (22 °C) for several hours. Samples used for uniaxial extension and radially confined compression were taken from the same film.

3. Results and discussion

Gel fractions ϕ and E of the prepared silicone blends are reported in Table 1. Values of ϕ measured in the undiluted samples agree well with those predicted in the diluted state. This suggests that tuning the sol fraction does not significantly alter the crosslinked network that forms and can be treated as a straightforward dilution of the network. A plot of E vs. ϕ for various mixing ratios (Fig. 3) indicates that $E \sim \phi^{2.83\pm0.28}$. Note that the values of E were measured at the same strain rate to avoid the influence of rate effects. This scaling exponent, while only observed with data spanning half a decade, may indicate a filler effect from the silica that is present in the commercial silicone kit. According to the Guth–Gold model, $E \sim E_M(\phi_F)^2$ where E_M is the modulus of the matrix and ϕ_F is the fraction of filler in the system [66]. Adding unreactive chains into a system with filler should cause a reduction in both E_M and ϕ_F which leads to a predicted scaling of $E \sim \phi^3$, close to the value of $E \sim \phi^{2.83\pm0.28}$ observed in experiment. Thus, the observed scaling of $E \sim \phi^{2.83\pm0.28}$ enables the isolation of the effect of crosslinking density from changes in sol fraction in the samples with varying mixing ratio.

Plots of K against E for samples that alter the volume fraction and the crosslinking density are shown in Fig. 4. Note that E was corrected for sol fraction effects, using the empirical scaling from Fig. 3 (shift factors reported in supplementary information), in Fig. 4b to isolate the effect of crosslinking density. An estimate of $K = 1.7$ GPa from Tabor's model, developed in the SI, is included on these plots. In both cases, K appears to systematically increase with volume fraction and crosslinking density. The data indicate that $K \sim E^{0.45\pm0.05}$ when altering volume fraction while $K \sim E^{0.28\pm0.05}$ when altering the crosslinking density. The observation that K depends on E when altering network structure shows that Tabor's model provides an incomplete understanding of K in nearly incompressible polymer networks. These results demonstrate that K is sensitive to both polymer volume fraction and network crosslinking density.

Measurements of E and K can be used to estimate ν using Eq. (1). For this, it is important to consider how uncertainty in the measurement of both E and K propagate to uncertainty in the value of ν [57]. Rearranging and including error in the measurement gives,

$$\Delta\nu = \frac{E}{6K}\sqrt{\left(\frac{\Delta E}{E}\right)^2 + \left(\frac{\Delta K}{K}\right)^2}, \tag{3}$$

where $\frac{\Delta E}{E}$ represents the relative uncertainty in the measurement of E. The form of this equation shows that any error in E and K is scaled by $\frac{E}{6K}$. Since E and K are orders of magnitude apart, large errors in the measurement of the moduli can translate to very small errors in ν. This insensitivity to errors in modulus measurement is why quantifying E and K offers such a high level of precision [57]. For example, if $K = 1$ GPa and $E = 1$ MPa then $\frac{E}{6K} = 1.\overline{6} \times 10^{-4}$ giving an exact value of $\nu = 0.4998\overline{3}$. Now assuming a ±25% error for both E and K gives $\Delta\nu = .00006$. This translates to 0.01% uncertainty in the value of ν, which means that this measurement would only be precise to the fourth decimal point and should be reported as $\nu = 0.4998$. Based on this argument, samples with a mixing ratio of 10:1 should be precise to the fourth decimal point while all other tested samples are precise to the fifth decimal point.

Plots of ν against E are shown in Fig. 5 for (a) altering volume fraction and (b) altering crosslinking density. Note that E has been shifted to isolate the effect of altering crosslinking density in Fig. 5b. An estimate of ν calculated using the value of $K = 1.7$ GPa from Tabor's model is also included on each plot. Each of the values at constant mixing ratio in Fig. 5a are only differentiated by the fifth decimal point. This indicates that the difference between these data is beyond the resolution limit of the measurement technique and so no scaling can be confidently extracted. Interestingly, predictions of the Tabor model are close to the observed values at different mixing ratios. The data sets in Fig. 5b are differentiated by the fourth decimal point and ν appears to be linearly dependent on E. However, the effect appears to be very slight, as a increasing E by two orders of magnitude only decreases ν by 0.04%. Together, these results indicate that ν is sensitive to crosslinking density and is largely insensitive to volume fraction, at least within the resolution limit of this technique.

It is interesting to note the agreement in both plots between the measured values of ν and those predicted using a constant value of K from Tabor's model. This agreement is a consequence of the insensitivity of ν to errors in the measurement of K relative to E, and suggests that while Tabor's model may be an incomplete description of K, it can be used to estimate ν in the nearly incompressible regime. The observed linear scaling of ν with E indicates a relative difference in the sensitivity of E and K to network structure. ν is proportional to $\frac{E}{K}$, and E shifts by two orders of magnitude as crosslinking density and volume fraction are altered in the blends. In comparison, K shifts by a factor of

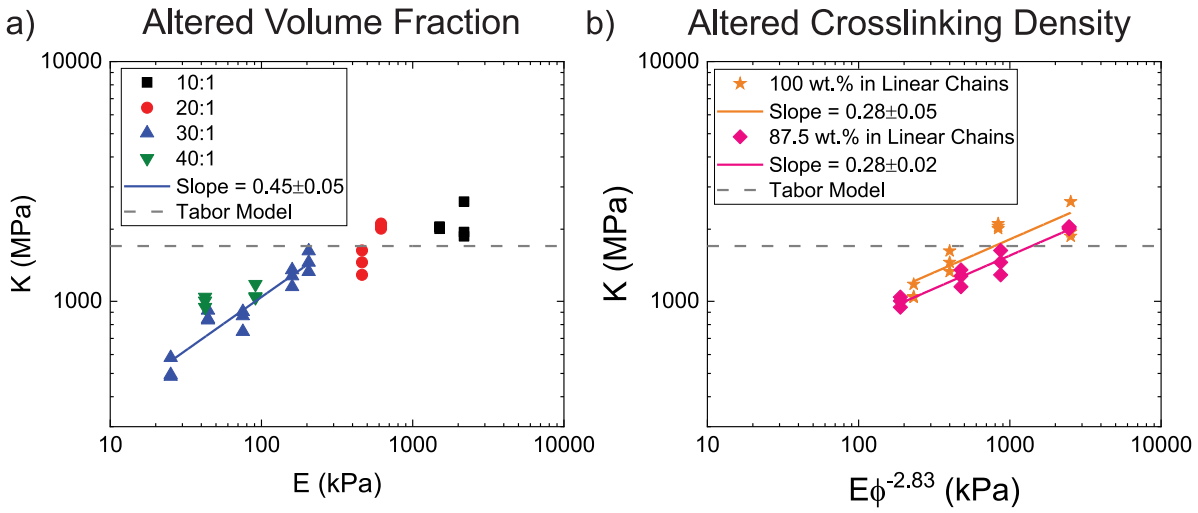

Fig. 4. (a) Plot of K against E in samples that alter volume fraction indicating that $K \sim E^{0.45\pm0.05}$. (b) Plot of K against $E\phi^{-2.83}$ in samples that alter crosslinking density indicating that $K \sim E^{0.28\pm0.05}$. This demonstrates that K is influenced by altering both the volume fraction and crosslinking density.

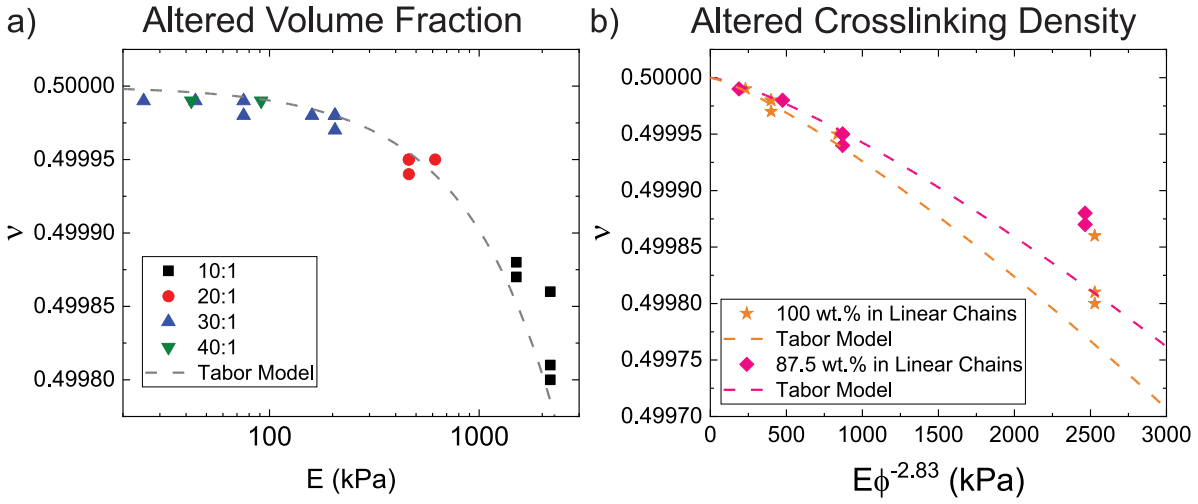

Fig. 5. (a) Plot of ν against E in samples that alter volume fraction with different crosslinking densities, indicated by mixing ratios. While differences in ν at each mixing ratio are not easily resolved, predictions of the Tabor model are close to the observed values at the different mixing ratios. (b) Plot of ν against $E\phi^{-2.83}$ in samples that alter crosslinking density, suggesting a linear dependence. This demonstrates that ν is both insensitive to volume fraction and sensitive to crosslinking density.

approximately 3 for the same samples. These relative sensitivities result in an apparent linear trend of ν with respect to E, even without correcting for changes in K.

Together these results demonstrate that the bulk modulus of an elastomer varies as the network structure is systematically altered by tuning both the crosslinking density and volume fraction. It was found that $K \sim E^{0.45\pm0.05}$ when altering the crosslinking density and $K \sim E^{0.28\pm0.05}$ when changing volume fraction. Notably, ν is less sensitive to network structure than K with only a slight reduction when altering the crosslinking density and an unresolvable difference when altering volume fraction. This shows that the current theoretical understanding of K in polymer networks is incomplete; however, it should be sufficient for estimating ν of nearly incompressible networks given the insensitivity of this property to errors in K.

While the results presented above illustrate a relationship between network structure and K in nearly incompressible polymer networks, it is important to discuss the limitations of these findings. First, the use of a commercial kit to create the silicone blends offers limited control over the network structure. The observation that fillers may play a role when altering the polymer volume fraction suggests that the influence of this filler may be a confounding variable for the scalings reported here. This is likely important given that changing the mixing ratio alters the sol fraction without dramatically changing the filler concentration. Performing similar measurements with a material system that offers greater molecular control is of interest in the future. Second, while bulk modulus appears to be sensitive to network structure, it is not immediately clear how varying volume fraction and crosslinking density alter K. We suspect that both decreasing the crosslinking density and increasing the diluent concentration increases the number of chain ends in the system which could lead to a reduction in the effective packing ratio that Tabor assumed to be an unrealistic, dense-packing FCC structure. Combining direct structural characterization, to measure a realistic packing structure in a material with more precise network control, with further measurements of bulk modulus to test modified versions of Tabor's model is of interest in the future.

4. Conclusions

Radially confined compression was used to quantify the bulk modulus of nearly incompressible polymer networks. It was

found that the bulk modulus systematically changes with both polymer volume fraction and crosslinking density. Poisson's ratio was found to be approximately insensitive to network volume fraction, and appears to linearly decrease as crosslinking density increased, which is a consequence of the relative difference in sensitivity to crosslinking density between Young's modulus and the bulk modulus. These results expand the experimental understanding of bulk modulus and present an opportunity to deepen the physical understanding of this property.

Declaration of competing interest

The authors declare that they have no known competing financial interests or personal relationships that could have appeared to influence the work reported in this paper.

Acknowledgments

This work was supported by the Materials Research Science and Engineering Center (MRSEC), United States Program of the National Science Foundation under Award No. DMR 1720256 (IRG–3). This work was performed within the research facilities within the California NanoSystems Institute, supported by the University of California, Santa Barbara and the University of California, Office of the President, and leveraged resources supported by the National Science Foundation, United States under Award No. DMR-1933487. The authors also acknowledge the use of instrumentation in the Mechanical Test Lab at the University of California Santa Barbara and thank Kirk Fields for helpful discussions regarding experimental protocol.

Appendix A. Supplementary data

Supplementary material related to this article can be found online at https://doi.org/10.1016/j.eml.2022.101616.

References

[1] P.J. Flory, Network structure and the elastic properties of vulcanized rubber, Chem. Rev. 35 (1) (1944) 51–75, http://dx.doi.org/10.1021/cr60110a002.
[2] F.T. Wall, Statistical thermodynamics of rubber. III, J. Chem. Phys. 11 (1943) 527, http://dx.doi.org/10.1063/1.1748098, URL http://aip.scitation.org/doi/10.1063/1.1748098.
[3] P.J. Flory, J. Rehner, Statistical mechanics of cross-linked polymer networks II. Swelling, J. Chem. Phys. 11 (11) (1943) 521–526, http://dx.doi.org/10.1063/1.1723792, arXiv:9809069v1.
[4] L.R.G. Treloar, Stress-strain data for vulcanised rubber under various types of deformation, Trans. Faraday Soc. 39 (241) (1943) 59–70.
[5] F.T. Wall, P.J. Flory, Statistical thermodynamics of rubber elasticity, J. Chem. Phys. 19 (12) (1951) 1435–1439, http://dx.doi.org/10.1063/1.1748098, URL http://aip.scitation.org/doi/10.1063/1.1748098.
[6] L.R.G. Treloar, The photoelastic properties of short-chain molecular networks, Trans. Faraday Soc. 50 (1954) 881–896, http://dx.doi.org/10.1039/tf9545000881.
[7] C.G. Moore, W.F. Watson, Determination of degree of crosslinking in natural rubber vulcanizates. Part II, J. Polymer Sci. XIX (1956) 237–254.
[8] L. Mullins, Determination of degree of crosslinking in natural rubber vulcanizates. Part iii., J. Appl. Polymer Sci. II (4) (1959) 1–7.
[9] S. Candau, A. Peters, J. Herz, Experimental evidence for trapped chain entanglements: Their influence on macroscopic behaviour of networks, Polymer 22 (11) (1981) 1504–1510,
[10] M. Rubinstein, Dynamics of ring polymers in the presence of fixed obstacles, Phys. Rev. Lett. 57 (24) (1986) 3023–3026, http://dx.doi.org/10.1103/PhysRevLett.57.3023.
[11] M. Rubinstein, S. Panyukov, Elasticity of polymer networks, Macromolecules 35 (17) (2002) 6670–6686, http://dx.doi.org/10.1021/ma0203849, arXiv:0303592.
[12] S.P. Obukhov, M. Rubinstein, R.H. Colby, Network modulus and superelasticity, Macromolecules 27 (12) (1994) 3191–3198, http://dx.doi.org/10.1021/ma00090a012, URL http://www.scopus.com/inward/record.url?eid=2-s2.0-0028766596&partnerID=40&md5=fa1e9f6e15ead25265b1abbb5c10663f.
[13] M. Zhong, R. Wang, K. Kawamoto, B.D. Olsen, J.A. Johnson, Quantifying the impact of molecular defects on polymer network elasticity, Science 353 (6305) (2016) 1264–1268, http://dx.doi.org/10.1126/science.aag0184, arXiv:arXiv:1011.1669v3, URL http://www.sciencemag.org/cgi/doi/10.1126/science.aag0184.
[14] P. Flory, Molecular theory of rubber elasticity, Polymer 17 (1) (1985) 1–12, http://dx.doi.org/10.1016/0032-3861(79)90268-4, URL http://www.sciencedirect.com/science/article/pii/0032386179902684.
[15] J.P. Gong, Y. Katsuyama, T. Kurokawa, Y. Osada, Double-network hydrogels with extremely high mechanical strength, Adv. Mater. 15 (14) (2003) 1155–1158, http://dx.doi.org/10.1002/adma.200304907, arXiv:79951804311.
[16] D.A. Davis, A. Hamilton, J. Yang, L.D. Cremar, D. Van Gough, S.L. Potisek, M.T. Ong, P.V. Braun, T.J. Martínez, S.R. White, J.S. Moore, N.R. Sottos, Force-induced activation of covalent bonds in mechanoresponsive polymeric materials, Nature 459 (7243) (2009) 68–72, http://dx.doi.org/10.1038/nature07970.
[17] Y. Okumura, K. Ito, The polyrotaxane gel: A topological gel by figure-of-eight cross-links, Adv. Mater. 13 (7) (2001) 485–487, http://dx.doi.org/10.1002/1521-4095(200104)13:7<485::AID-ADMA485>3.0.CO;2-T.
[18] L.H. Cai, T.E. Kodger, R.E. Guerra, A.F. Pegoraro, M. Rubinstein, D.A. Weitz, Soft poly(dimethylsiloxane) elastomers from architecture-driven entanglement free design, Adv. Mater. 27 (35) (2015) 5132–5140, http://dx.doi.org/10.1002/adma.201502771.
[19] D. Tabor, The bulk modulus of rubber, Polymer 35 (13) (1994) 2759–2763.
[20] A.N. Gent, P.B. Lindley, The compression of bonded rubber blocks, Proc. Inst. Mech. Eng. 173 (1) (1959) 111–122.
[21] A.N. Gent, E. Meinecke, Compression, bending, and shear of bonded rubber blocks, Polymer Eng. Sci. 10 (1) (1970) 48–53.
[22] P.B. Lindley, Compression moduli for blocks of rigid end plates, J. Strain Anal. 14 (1) (1979) 11–16.
[23] Y.-H. Lai, D.A. Dillard, J.S. Thornton, The effect of compressibility on the stress distributions in thin elastomeric blocks and annular bushings, J. Appl. Mech. Trans. ASME 60 (3) (1992) 787, http://dx.doi.org/10.1115/1.2900878.
[24] K.R. Shull, D. Ahn, W.-L. Chen, C.M. Flanigan, A.J. Crosby, Axisymmetric adhesion tests of soft materials, Macromol. Chem. Phys. 199 (4) (1998) 489–511, http://dx.doi.org/10.1002/macp.1998.021990402, URL http://doi.wiley.com/10.1002/(SICI)1521-3935(19980401)199:4%3C489::AID-MACP489%3E3.0.CO;2-A.
[25] R. Hensel, R.M. McMeeking, A. Kossa, Adhesion of a rigid punch to a confined elastic layer revisited, J. Adhesion 95 (1) (2019) 44–63, http://dx.doi.org/10.1080/00218464.2017.1381603.
[26] A.N. Gent, P. Lindley, Internal rupture of bonded rubber cylinders in tension, Proc. R. Soc. Of London Ser. A 249 (1257) (1959) 195–205.
[27] C.W. Barney, C.E. Dougan, K.R. Mcleod, A. Kazemi-moridani, Y. Zheng, Z. Ye, S. Tiwari, I. Sacligil, R.A. Riggleman, S. Cai, J.-H. Lee, S.R. Peyton, G.N. Tew, A.J. Crosby, Cavitation in soft matter, Proc. Nat. Acad. Sci. 117 (17) (2020) 9157–9165, http://dx.doi.org/10.1073/pnas.1920168117,
[28] J.A. Zimberlin, N. Sanabria-DeLong, G.N. Tew, A.J. Crosby, Cavitation rheology for soft materials, Soft Matter 3 (6) (2007) 763, http://dx.doi.org/10.1039/b617050a.
[29] S. Kundu, A.J. Crosby, Cavitation and fracture behavior of polyacrylamide hydrogels, Soft Matter 5 (20) (2009) 3963, http://dx.doi.org/10.1039/b909237d, URL http://pubs.rsc.org/en/content/articlehtml/2009/sm/b909237d.
[30] S.B. Hutchens, S. Fakhouri, A.J. Crosby, Elastic cavitation and fracture via injection, Soft Matter 12 (2016) 2557–2566, http://dx.doi.org/10.1039/C5SM02055G.
[31] C.W. Barney, Y. Zheng, S. Wu, S. Cai, A.J. Crosby, Residual strain effects in needle-induced cavitation, Soft Matter 15 (37) (2019) 7390–7397, http://dx.doi.org/10.1039/C9SM01173K, URL http://pubs.rsc.org/en/Content/ArticleLanding/2019/SM/C9SM01173K.
[32] C.W. Barney, C. Chen, A.J. Crosby, Deep indentation and puncture of a rigid cylinder inserted into a soft solid, Soft Matter 17 (22) (2021) 5574–5580, http://dx.doi.org/10.1039/d0sm01775b.
[33] Z. Laufer, Y. Diamant, M. Gill, G. Fortuna, A simple dilatometric method for determining Poisson ' s ratio of nearly incompressible elastomers, Int. J. Polymeric Mater. 6 (3–4) (1978) 159–174, http://dx.doi.org/10.1080/00914037808077906.
[34] R.J. Farris, Dilatation of granular filled elastomers under high rates of strain, J. Appl. Polymer Sci. 8 (1964) 25–35.
[35] U. Yilmazer, R.J. Farris, Mechanical behavior and dilatation of particulate-filled thermosets in the rubbery state, J. Appl. Polymer Sci. 28 (1983) 3369–3386.
[36] R.J. Farris, The influence of vacuole formation on the response and failure of filled elastomers, Trans. Soc. Rheol. 12 (2) (1968) 315–334, http://dx.doi.org/10.1122/1.549111.
[37] H.F. Schippel, Volume increase of compounded rubber under strain, J. Ind. Eng. Chem. 12 (1) (1920) 33–37.

[38] H.C. Jones, H.A. Yiengst, Dilatometer studies of pigment- rubber systems, Ind. Eng. Chem. 32 (10) (1940) 1354–1359.
[39] R. Shuttleworth, Volume change measurements in the study of rubber-filler interactions, Eur. Polym. J. 4 (1) (1968) 31–38, http://dx.doi.org/10.1016/0014-3057(68)90005-0.
[40] T.L. Smith, Volume changes and dewetting in glass bead-polyvinyl chloride elastomeric composites under large deformations, Trans. Soc. Rheol. 3 (1) (1959) 113–136, http://dx.doi.org/10.1122/1.548847.
[41] J.C. Smith, G.A. Kermish, C.A. Fenstermaker, Separation of filler particles from the matrix in a particulate-loaded composite subjected to tensile stress, J. Adhesion 4 (2) (1972) 109–122, http://dx.doi.org/10.1080/00218467208072216.
[42] W. Ren, P.J. McMullan, A.C. Griffin, Poisson's ratio of monodomain liquid crystalline elastomers, Macromol. Chem. Phys. 209 (18) (2008) 1896–1899, http://dx.doi.org/10.1002/macp.200800265.
[43] Y.-X. Xu, J.-Y. Juang, Measurement of nonlinear Poisson's ratio of thermoplastic polyurethanes under cyclic softening using 2D digital image correlation, Polymers 13 (2021) 1498.
[44] L.I. Farfan-Cabrera, J.B. Pascual-Francisco, O. Barragan-Perez, E.A. Gallardo-Hernandez, O. Susarrey-Huerta, Determination of creep compliance, recovery and Poisson's ratio of elastomers by means of digital image correlation (DIC), Polym. Test. 59 (2017) 245–252, http://dx.doi.org/10.1016/j.polymertesting.2017.02.010.
[45] R.H. Pritchard, P. Lava, D. Debruyne, E.M. Terentjev, Precise determination of the Poisson ratio in soft materials with 2D digital image correlation, Soft Matter 9 (26) (2013) 6037–6045.
[46] R.H. Pritchard, E.M. Terentjev, Swelling and de-swelling of gels under external elastic deformation, Polymer 54 (26) (2013) 6954–6960, http://dx.doi.org/10.1016/j.polymer.2013.11.006.
[47] S. Dogru, B. Aksoy, H. Bayraktar, B.E. Alaca, Poisson's ratio of PDMS thin films, Polym. Test. 69 (2018) 375–384, http://dx.doi.org/10.1016/j.polymertesting.2018.05.044.
[48] C. Weir, Temperature dependence of compression of natural rubber-sulfur vulcanizates of high sulfur content, J. Res. Nat. Bureau Standards 50 (3) (1953) 153, http://dx.doi.org/10.6028/jres.050.024.
[49] L.H. Adams, R.E. Gibson, The compressibility of rubber, J. Washington Acad. Sci. 20 (12) (1930) 213–223, http://dx.doi.org/10.5254/1.3535518.
[50] L.A. Wood, G.M. Martin, Compressibility of natural rubber at pressures below 500 KG/CM2, Rubber Chem. Technol. 37 (4) (1964) 850–865, http://dx.doi.org/10.5254/1.3540383.
[51] S.H. Cho, G. Kim, T.J. McCarthy, R.J. Farris, Orthotropic elastic constants for polyimide film, Polymer Eng. Sci. 41 (2) (2001) 301–307, http://dx.doi.org/10.1002/pen.10729.
[52] R. Feng, R.J. Farris, The characterization of the thermal and elastic constants for an epoxy photoresist SU8 coating, J. Mater. Sci. 37 (2002) 4793–4799.
[53] A.H. Scott, Specific volume, compressibility, and volume thermal expansivity of rubber-sulfur compounds, J. Res. Nat. Bureau Standards 14 (1935) 99–120.
[54] L.E. Copeland, The thermodynamics of a strained elastomer. II. Compressibility, J. Appl. Phys. 19 (5) (1948) 445–449, http://dx.doi.org/10.1063/1.1698153.
[55] K.L. Fishman, D. Machmer, Testing techniques for measurement of bulk modulus, J. Testing Eval. 22 (2) (1994) 161–167, http://dx.doi.org/10.1520/jte12650j.
[56] G.K. Rightmire, An experimental method for determining Poisson's ratio of elastomers, J. Lubrication Technol. 92 (3) (1970) 381–386.
[57] M. Stanojevic, G.K. Lewis, A comparison of two test methods for determining elastomer physical properties, Polym. Test. 3 (1983) 183–195.
[58] G.A. Tizard, D.A. Dillard, A.W. Norris, N. Shephard, Development of a high precision method to characterize Poisson's ratios of encapsulant gels using a flat disk configuration, Exp. Mech. 52 (2012) 1397–1405, http://dx.doi.org/10.1007/s11340-011-9589-6.
[59] B.P. Holownia, Effect of carbon black on Poisson's ratio of elastomers, Rubber Chem. Technol. 48 (2) (1975) 246–253.
[60] J.N. Farber, R.J. Farris, Model for prediction of the elastic response of reinforced materials over wide ranges of concentration, J. Appl. Polymer Sci. 34 (6) (1987) 2093–2104, http://dx.doi.org/10.1002/app.1987.070340604.
[61] N.W. Tschoegl, W.G. Knauss, I. Emri, Poisson's ratio in linear viscoelasticity - a critical review, Mech. Time-Dependent Mater. 6 (1) (2002) 3–51, http://dx.doi.org/10.1023/A:1014411503170.
[62] Y. Hu, X. Zhao, J.J. Vlassak, Z. Suo, Using indentation to characterize the poroelasticity of gels, Appl. Phys. Lett. 96 (12) (2010) 2008–2011, http://dx.doi.org/10.1063/1.3370354.
[63] L. Garrido, J.E. Mark, J.L. Ackerman, R.A. Kinsey, Studies of self -difision of poly(dimethylsiloxane) chains in pdms model networks by pulsed field gradient NMR, J. Polymer Sci. Part B 26 (11) (1988) 2367–2377.
[64] K. Efimenko, W.E. Wallace, J. Genzer, Surface modification of sylgard-184 poly(dimethyl siloxane) networks by ultraviolet and ultraviolet/ozone treatment, J. Colloid Interface Sci. 254 (2) (2002) 306–315, http://dx.doi.org/10.1006/jcis.2002.8594.
[65] D. Ortiz-Acosta, C. Densmore, Sylgard® Cure Inhibition Characterization, Tech. rep., Los Alamos National Laboratory, 2012, http://dx.doi.org/10.2172/1053123, URL https://permalink.lanl.gov/object/tr?what=info%3Alanl-repo%2Flareport%2FLA-UR-12-25325.
[66] E. Guth, Theory of filler reinforcement, J. Appl. Phys. 16 (1) (1945) 55, http://dx.doi.org/10.1063/1.1707501.